

Verification Benchmark Analysis of Structural Reliability Evaluation Codes for Fast Reactor Components

Shigeru TAKAYA^{1,*}, Naoto SASAKI², Toshiki OKAMOTO³ and Hideo MACHIDA³

¹Japan Atomic Energy Agency, 4002 Narita, Oarai, Ibaraki 311-1393, Japan

²Ascend Co., Ltd., 4002 Narita, Oarai, Ibaraki 311-1313, Japan

³TEPCO Systems Corporation, 2-37-28 Eitai, Koto-ku, Tokyo 135-0034, Japan

ABSTRACT

This paper describes benchmark analysis of independently programmed structural reliability evaluation codes, REAL-P and GENPEP. An upper core structure of a prototype fast breeder reactor in Japan, MONJU, was chosen, and crack initiation time and crack propagation due to fatigue-creep interaction damage was evaluated in deterministic and probabilistic manners. Evaluation procedures follow the new guidelines on reliability evaluation of fast reactor components issued by JSME. The results obtained by two codes were compared, and the effects of differences in treatments of which details are not prescribed in the guidelines on results were discussed. As result, although slight difference was recognized in crack initiation evaluation especially due to difference in fairing treatment of fatigue life curves, the results estimated by two codes generally agreed very well for both deterministic and probabilistic evaluations. It was shown that the effects of differences in treatments of which details are not prescribed in the guidelines on results are small for structural reliability evaluation of fatigue-creep interaction damage, which is one of typical degradation mechanisms for fast reactor passive components.

KEYWORDS

System Based Code concept, Inservice inspection, Fatigue-creep interaction damage, Crack initiation, Crack propagation, Deterministic evaluation, Probabilistic evaluation, Plant safety

ARTICLE INFORMATION

Article history:

Received 22 October 2018

Accepted 04 February 2020

1. Introduction

A new code case on inservice inspection (ISI) requirements for sodium-cooled fast reactor passive components was issued in the American Society of Mechanical Engineers (ASME) boiler and pressure vessel code [1]. The code case was developed by a joint task group between ASME and the Japan Society of Mechanical Engineers (JSME) based on the System Based Code concept that pursues improvements in reliability and economy while meeting plant safety goals [2]. The code case provides a flow to determine ISI requirements which consists of two stages. The first stage focuses on structural integrity of components. Potential active degradation mechanisms are considered based on conditions including material and service environment, and then reliability of the specified component that is a complement of failure probability is evaluated. If the reliability meets a target value, it is possible to proceed to the next stage, where plant safety is focused on. An assessment is made of the detectability of defects before they grow to an unacceptable size in consideration of plant safety. If there is any feasible way to reliably detect degradation, it is adapted as ISI. Otherwise, a structural integrity evaluation would be required while employing a sufficiently conservative hypothesis. If the result meets the target value, ISI is not obligation. In this way, the proposed flow can determine ISI suitable to fast reactors by taking key characteristics including material, environment, inspection property and importance of components in light of plant safety into consideration.

Thus, structural reliability evaluation plays an important role to determine suitable ISI requirements according to the code case. Therefore, a mandatory appendix for procedure for structural reliability evaluation for passive components is included in the code case. Correspondingly, JSME has published guidelines on reliability evaluation of fast reactor components [3]. In addition to the

*Corresponding author, E-mail: takaya.shigeru@jaea.go.jp

guidelines, development of structural reliability evaluation codes which can conduct evaluations following the guidelines is also needed. Furthermore, it is important to confirm the effects of differences in treatments of which details are not prescribed in the guidelines on results.

Therefore, in this paper, benchmark analysis on crack initiation and propagation due to fatigue-creep interaction damage, which is one of typical degradation mechanisms for fast reactor passive components, was conducted by using independently programmed codes, REAL-P and GENPEP [4]. In sodium-cooled fast reactors, internal pressure is much lower than light-water-reactors because of high boiling temperature of sodium while thermal stress is high due to relatively large temperature changes during start-ups and shutdowns. In addition, evaluation of stress relaxation behavior at elevated temperature is important. Both codes were developed to deal with these features of sodium-cooled fast reactors in the ways following the guidelines.

2. Evaluation Procedures

Evaluation procedures of fatigue-creep interaction damage followed the guidelines on reliability evaluation of fast reactor components [3]. As for crack initiation evaluation, fatigue damage, D_f , and creep damage, D_c , were calculated respectively, and it was assumed that a crack initiated when D_f and D_c met the following equation;

$$D = f(D_f, D_c) \quad (1)$$

where D is the critical value that connects points $(D_f, D_c) = (1, 0), (0.3, 0.3),$ and $(0, 1)$. As for crack propagation evaluation, the following equation was used;

$$\frac{da}{dn} = C_f \Delta J_f^{m_f} + \int_{1 \text{ cycle}} C_c J_c^{m_c} dt \quad (2)$$

where a is the crack depth, and C_f, C_c, m_f and m_c are material constants. ΔJ_f is J-integral range for fatigue crack growth evaluation and J_c is J-integral for creep crack growth evaluation. ΔJ_f was evaluated by the procedures explained in Ref. [9] which is also employed in the guidelines. More details in the procedures are explained somewhere [3, 5, 9].

An upper core structure (UCS) of a prototype fast breeder reactor in Japan, MONJU, was chosen as a target component for this benchmark analysis (Fig. 1). Initiation and propagation of a crack on the outer surface of the shroud at the sodium surface level during normal operations were evaluated. As for the crack propagation evaluation, a full circumferential crack with the depth of 1 mm was assumed as an initial crack. Analysis conditions were determined as shown in Table 1, based on a previous study conducting a hypothetical evaluation without a stress-relief structure of the shroud [6]. As mentioned above, the steady primary stress due to internal pressure and dead weight was small, and the thermal transient stress due to start-ups and shutdowns, which was corresponding to stress intensity range and secondary bending stress range in the vertical direction to the crack, was dominant. In addition, probabilistic distributions of random variables were also set as shown in Table 2, based on previous reports on statistical properties of material strength [7-9]. The thermal stress amplification factor, χ , was also employed as a random variable to consider potential scattering of temperature range during start-ups and shutdowns. This factor was multiplied by cyclic stress range and axial direction stress ranges in Table 1. α_R, α_c and α_f are random variables to consider variations of creep rupture time, steady-state creep strain rate and fatigue strength. Creep rupture time and fatigue strength used in probabilistic evaluations were obtained by dividing their mean values by α_R and α_f , respectively. Steady-state creep strain rate is a function of creep rupture time, and gets higher for shorter creep rupture time. The creep rupture time used for calculating steady-state creep strain rate was obtained by dividing the mean value by α_c . As for material constants in Eq. (2), the coefficients, C_f and C_c , were chosen as random variables while the exponents, m_f and m_c , were dealt deterministically. This was because variations of the coefficients were much larger than those of exponents in experiment results [9], and were considered to have dominant effect on variations of crack propagation rates. Values of m_f and m_c were 1.374 and 0.9069, respectively. In this study, both deterministic evaluation and probabilistic evaluation were conducted. As for probabilistic evaluation, not only a case where the whole set of random variables in Table 2 was considered but also cases where only some of them were selected were prepared for detailed comparison of the codes as shown

in Table 3. Median values in Table 2 were used in the probabilistic evaluation if the parameters were not chosen as random variables in the case, as well as the deterministic evaluation.

Both REAL-P and GENPEP employed direct sampling Monte-Carlo method which is the most basic sampling method. The total sampling numbers are 10^4 for both REAL-P and GENPEP.

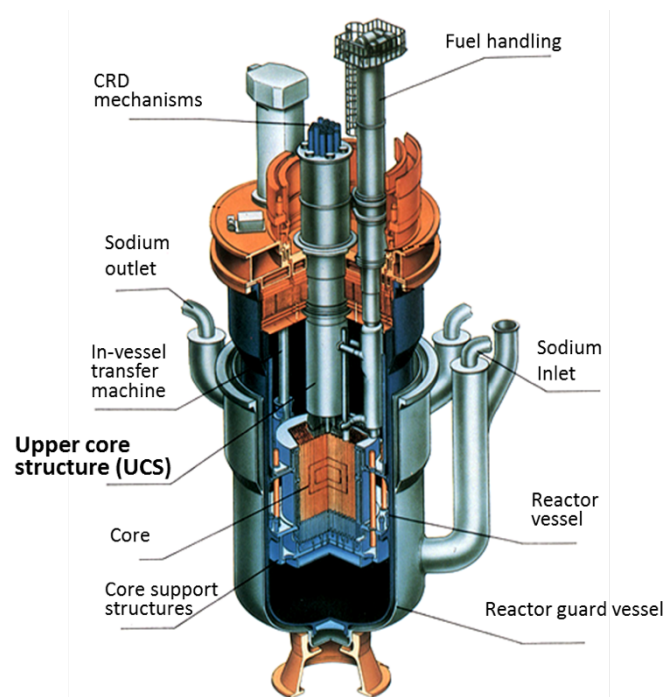


Fig. 1 Reactor structure of Monju

Table 1 Evaluation Parameters

Parameter	Value	
Material	304SS	
Outer diameter (mm)	1875	
Wall thickness (mm)	60	
Operating temperature (°C)	530	
Temperature in cold shutdown state (°C)	200	
Total duration at elevated temperature (h)	210000	
Temperature range for calculation of peak thermal strain range (°C)	5	
Steady primary stress (MPa)	1	
Stress intensity range* (MPa)	350	
Stress range in the vertical direction to the crack (MPa)	Primary membrane	0
	Primary bending	0
	Secondary membrane	0
	Secondary bending	175
Shakedown range (MPa)	215	
Strain rate (mm/mm/s)	1×10^{-8}	
Number of cycles per 30 years	460	

*: The range of stress during a loading cycle

Table 2 List of Random Variables

Random Variable	Distribution type	Median	Logarithmic standard deviation
Thermal stress amplification factor, χ (-)	Log-normal	1.00	0.078
Creep rupture time reduction factor, α_R (-)	Log-normal	1.00	0.560
Creep strain amplification factor, α_c (-)	Log-normal	1.00	0.800
Fatigue life reduction factor, α_f (-)	Log-normal	0.10	0.420
Coefficient for creep crack growth, C_c ($\text{mm}^{m_c+1} \cdot \text{h}^{m_c-1} / \text{N}^{m_c}$)	Log-normal	1.59×10^{-2}	0.422
Coefficient for fatigue crack growth, C_f ($\text{mm}^{m_f+1} / \text{N}^{m_f}$)	Log-normal	6.34×10^{-5}	0.422

Table 3 Analysis Cases of Probabilistic Evaluation

	Selected random variable(s)	Remarks
Case 1	$\chi, \alpha_R, \alpha_c, \alpha_f, C_c, C_f$	<ul style="list-style-type: none"> All of the random variables in Table 2 are considered.
Case 2	χ	<ul style="list-style-type: none"> Only a random variable related to stress is considered.
Case 3	$\alpha_R, \alpha_c, \alpha_f$	<ul style="list-style-type: none"> Only random variables related to material properties except coefficients for crack propagation are considered. α_R and α_f are not used in crack propagation evaluation.
Case 4	C_c, C_f	<ul style="list-style-type: none"> Only coefficients for crack propagation are considered. Both parameters are not used in crack initiation evaluation.

3. Results and Discussion

Tables 4 and 5 show comparison of deterministic evaluation results of crack initiation and crack propagation, respectively. It should be noted again that they are results in the hypothetical condition without a stress-relief structure. In both cases, REAL-P and GENPEP gave similar results, of which difference is less than a few percentages.

A main reason of the slight difference of fatigue damage in Table 4 is whether fairing treatment of fatigue life curves was conducted or not. The guidelines recommend to use best-fit curves of fatigue life in the JSME code for design and construction of fast reactors (JSME FR code) [10] lowered by a factor of two for strain or 10 for cycles, whichever is more conservative, as average fatigue life curves for reliability evaluation [3]. However, the guidelines do not mention the fairing treatment. REAL-P conducted fairing treatment between these two curves as shown in Fig. 2 to prevent discontinuous change in fatigue life while GENPEP did not to avoid additional conservativeness. Therefore, REAL-P tended to give slight conservative fatigue damage in a certain strain range. Fatigue life curves are not used in crack propagation evaluation, so the difference of fatigue crack propagation in Table 5 is smaller than that of fatigue damage in Table 4.

On the other hand, as for creep, GENPEP gave slightly conservative results for both creep damage and creep crack propagation. These parameters are sensitive to stress relaxation behaviors. The guidelines provide the evaluation procedure of stress relaxation, but do not prescribe specific conditions as for time steps. As a result of comparison of treatments in two codes, it was found that REAL-P determined time steps in the same manner as the JSME FR code, while GENPEP employed an original manner. Schematic explanation of the manner used by REAL-P is shown in Fig. 3. Time step width was determined so that stress relaxation for one time step did not exceed the limit, $\Delta\sigma_{\max}$ (= 0.49 MPa). The default time step width for the first time step was 10^{-4} h, and those for time steps after the second time step were determined by dividing holding time at elevated temperature equally on the logarithmic axis: 20 parts for one order. If the calculated stress relaxation for one time step exceeded the limit, recalculation would be conducted by shortening the time step width by half. On the other hand, GENPEP determined a tentative time step width so that stress relaxation from initial stress for one time step became smaller than 0.1 MPa, and then one hundredth of the tentative time step width

or 10^{-5} h, whichever was shorter was chosen a final time step width. The same time step width were used for whole holding time at elevated temperature. The time step width used in GENPEP was shorter than that used in REAL-P. Furthermore, there was also a minor difference in the way of calculation of creep damage for each time step, d_c , which is expressed analytically by Eq. (3).

$$d_c = \int \frac{1}{t_r(\sigma)} dt \quad (3)$$

where t_r , σ and t are creep rupture time, stress and time, respectively. REAL-P actually evaluated d_c discretely by using Eq. (4) while GENPEP used Eq. (5).

$$d_c = \frac{1}{t_r(\sigma(t_0))} \frac{\Delta t}{2} + \frac{1}{t_r(\sigma(t_0 + \Delta t))} \frac{\Delta t}{2} \quad (4)$$

$$d_c = \frac{1}{t_r(\sigma(t_0))} \Delta t \quad (5)$$

where t_0 and Δt are time at the start point of each time step and time step width, respectively. These differences in treatments were considered to result in the difference of a few percentages as for creep damage and creep crack propagation.

Table 4 Comparison of deterministic evaluation results of crack initiation

Parameter	REAL-P: A	GENPEP: B	(A-B)/A (%)
Fatigue damage at the first cycle (-)	2.03×10^{-3}	1.99×10^{-3}	1.97
Creep damage at the first cycle (-)	5.19×10^{-3}	5.31×10^{-3}	-2.31
Crack initiation time (years)	8.35	8.41	-0.72

Table 5 Comparison of deterministic evaluation results of crack propagation

Parameter	REAL-P: A	GENPEP: B	(A-B)/A (%)
Fatigue crack propagation at the first cycle (mm)	3.75×10^{-5}	3.75×10^{-5}	0.00
Creep crack propagation at the first cycle (mm)	4.10×10^{-5}	4.19×10^{-5}	-2.20
Time for crack to reach half of wall thickness (years)	1.50×10^3	1.48×10^3	1.33

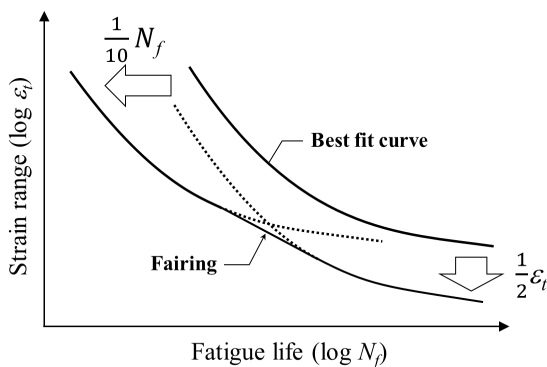


Fig.2 Fairing treatment of fatigue life curves (Schematic)

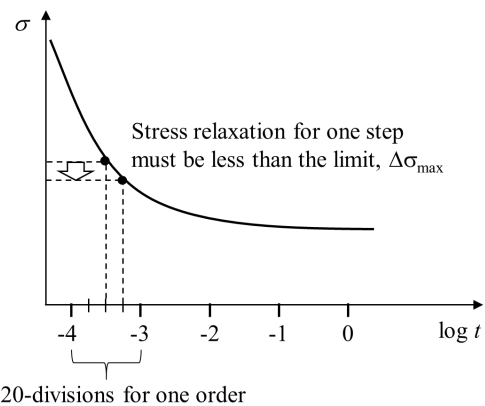


Fig.3 Determination of time steps for evaluation of stress relaxation (REAL-P)

Figure 4 shows comparison of accumulated crack initiation probability distributions evaluated by REAL-P and GENPEP. Those of Case 1 (Fig. 4(a)) where the whole set of random variables in Table 2 was considered agree well although there is very slight difference in the range above the accumulated probability of about 50%. This tendency is more apparent in Case 2 (Fig. 4(b)) while such difference is not recognized in Case 3 (Fig. 4(c)).

Figure 5 shows comparison of accumulated probability distributions of fatigue and creep damages at the first cycle evaluated by REAL-P and GENPEP in Case 2. Lower damage regions in Fig. 5 correspond to longer life regions in Fig. 4. Slight difference is recognized in a low damage region for the accumulated probability distributions of fatigue damage (Fig. 5(a)) while the distributions agree very well for creep damage (Fig. 5(b)). Therefore, it can be seen that this difference in fatigue damage causes the difference shown in Fig. 4(b). As explained above, there was a minor difference in fatigue damage evaluation between two codes. In order to examine the effect of this difference regarding fairing treatment, analytically evaluated accumulated probabilities are plotted in Fig. 5(a). Case 2 treated only one random variable, which enables to analytical evaluation. The plots coincide with corresponding curves, which means that the difference regarding fairing treatment is a main reason of the differences recognized in Fig. 5(a) and also Fig. 4(b). In the contrast, as for creep damage, very slight difference in the region where the accumulated probability is higher than approximately 50% was recognized. It is considered to be due to the difference in detailed evaluation procedures of stress relaxation behavior and creep damage discussed above. The influence of this difference in creep damage to the accumulated crack initiation probability was too small to be recognized in Figure 4.

In Case 3 (Fig. 4(c)), the effect of difference regarding fairing treatment of fatigue life curves was hardly recognized. It is because the fatigue life reduction factor, α_f , was chosen as a random variable in Case 3, and then an intersection point and a fairing region of two fatigue life curves illustrated in Fig. 2 moved from a strain range concerned in the evaluation.

As results, it was found that the both codes generally gave very similar results on crack initiation probability except for the very slight difference due to the fairing treatment of fatigue life curves.

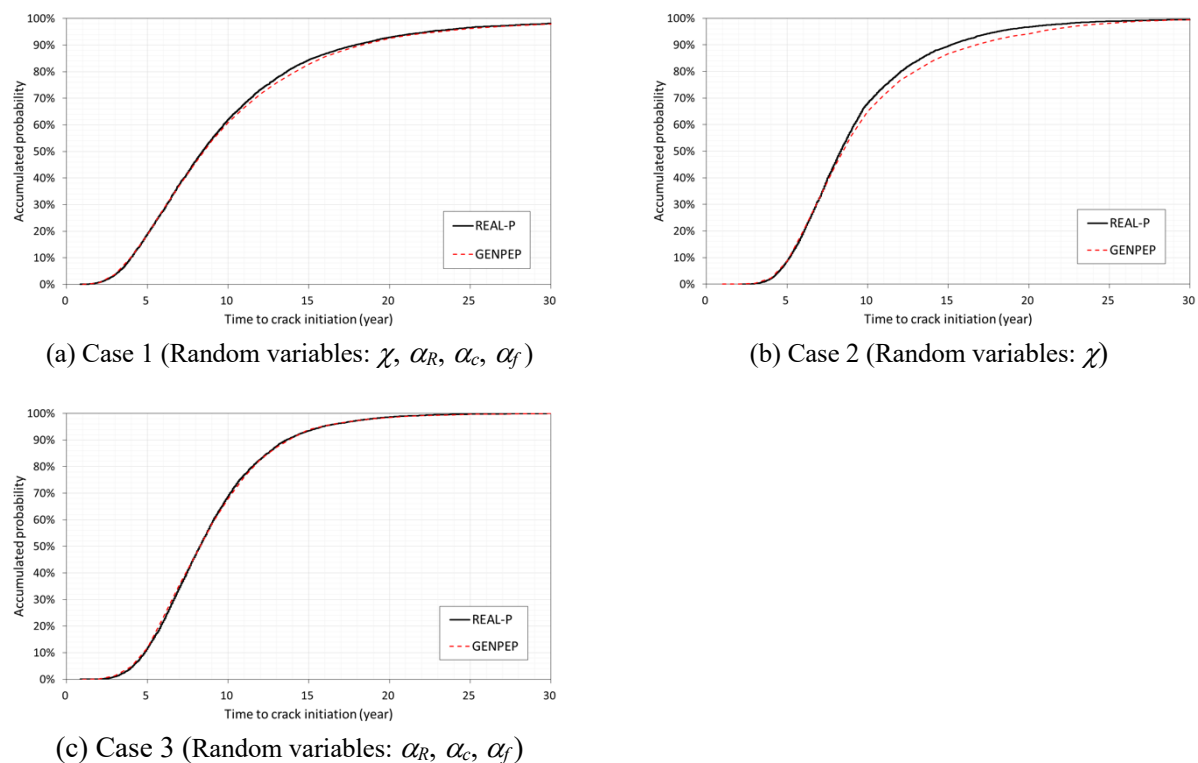
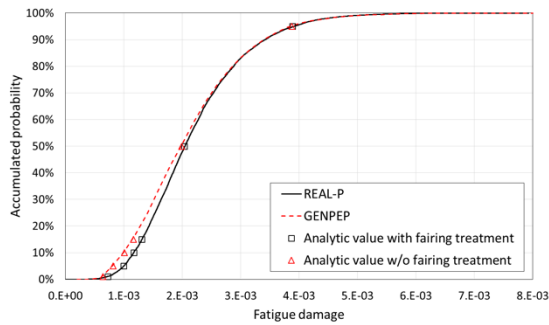
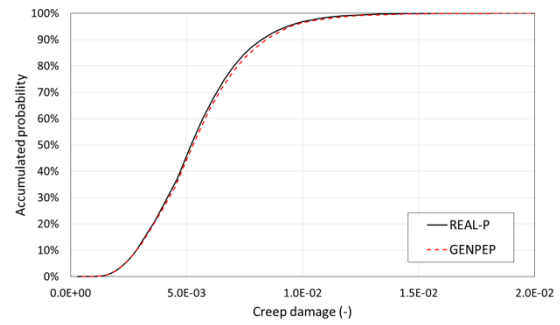


Fig. 4 Comparison of crack initiation probabilities evaluated by REAL-P and GENPEP



(a) Fatigue damage at the first cycle



(b) Creep damage at the first cycle

Fig. 5 Comparison of damage probabilities evaluated by REAL-P and GENPEP (Case 2)

Figure 6 shows comparison of accumulated crack propagation probability distributions at the first cycle. In every case, distributions evaluated by REAL-P and GENPEP agreed very well. Fatigue life curves are not used in the evaluation of crack propagation, so there is no influence of fairing treatment. In Cases 2 and 3 where just one random variable is considered, analytically calculated accumulated probabilities are also plotted, and the plots coincide curves evaluated by the two codes. It can be considered that both codes were programmed properly. As for the probabilistic evaluation of crack propagation, difference in results which required detailed discussion on treatments in the codes was not especially recognized.

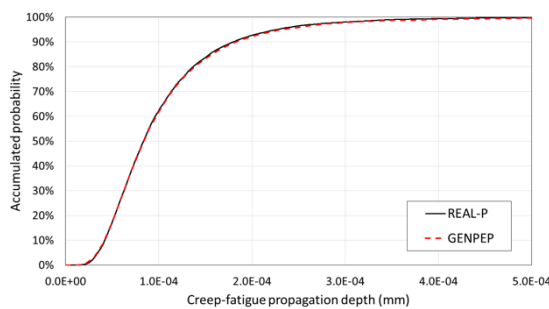
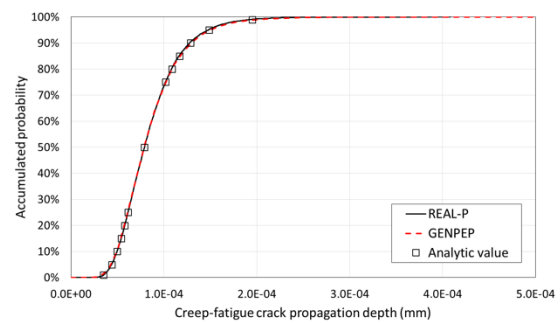
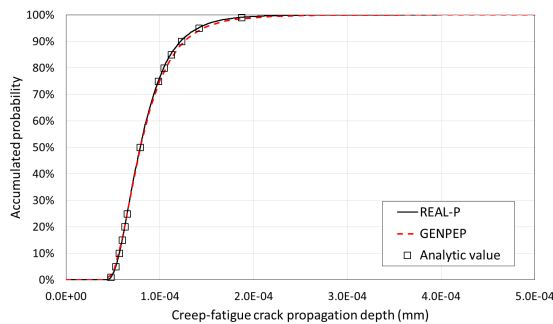
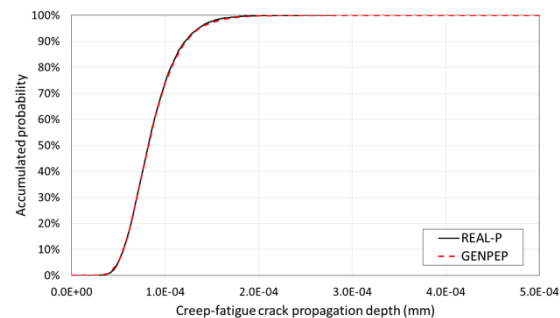

 (a) Case 1 (Random variables: χ , α_c , C_c , C_f)

 (b) Case 2 (Random variables: χ)

 (c) Case 3 (Random variables: α_c)

 (d) Case 4 (Random variables: C_c , C_f)

Fig. 6 Comparison of crack propagation probabilities at the first cycle evaluated by REAL-P and GENPEP

4. Conclusion

Structural reliability evaluation plays one of key roles to determine suitable ISI requirements of

sodium-cooled fast reactor passive components in the code case N-875 newly issued by ASME. JSME also has published new guidelines on reliability evaluation of fast reactor components. Thus, the importance of structural reliability evaluation is increasing.

In this study, a set of benchmark analysis conditions was prepared by using information of UCS of MONJU for verification of structural reliability evaluation codes. Deterministic and probabilistic evaluations of crack initiation and propagation due to creep-fatigue interaction damage, which is one of typical degradation mechanism for fast reactor components, were conducted by using independently developed structural reliability evaluation codes, REAL-P and GENPEP. There were several differences in treatments of which details are not mentioned in the guidelines such as fairing treatment of fatigue life curves and determination of time step for evaluation of stress relaxation, between two codes. Slight difference was recognized in crack initiation evaluation especially due to the difference in fairing treatment of fatigue life curves. However, in general, the results agreed very well. As a result, it is shown that the effects of differences in treatments of which details are not prescribed in the guidelines on results are small for structural reliability evaluation of fatigue-creep interaction damage, which is one of typical degradation mechanisms for fast reactor passive components.

It is also expected to use the set of input and output data presented in this paper for verification of other codes. Verification benchmark analysis of these codes will be also continued by increasing examples.

Acknowledgement

Present study includes the results of the “Technical development program on a commercialized FBR plant” entrusted to Japan Atomic Energy Agency (JAEA) by the Ministry of Economy, Trade and Industry of Japan (METI).

References

- [1] Case N-875 Alternative inservice inspection requirements for liquid-metal reactor passive components, 2017 ASME Boiler & Pressure Vessel Code, Code Cases: Nuclear Components Supplement 1 (2017).
- [2] Y. Asada, M. Tashimo and M. Ueta, System based code –Principal concept–, Proceedings of 10th International Conference on Nuclear Engineering, ID: ICONE10-22730 (2002).
- [3] JSME S NX7-2017 Guidelines on reliability evaluation of fast reactor components (2019), *in Japanese*.
- [4] S. Yoshimura and Y. Kanto eds., Probabilistic fracture mechanics for risk-informed activities –Fundamentals and Applications–, The Japan Welding Engineering Society (2017). <http://www-it.jwes.or.jp/ae/free/ae-1402e/ae-1402e-00.pdf>
- [5] S. Takaya, Y. Kamishima, H. Machida, D. Watanabe and T. Asayama, Determination of in-service inspection requirements for fast reactor components using System Based Code concept, Nuclear Engineering and Design, Vol. 305, pp.270-276 (2016).
- [6] S. Takaya, T. Asayama, Y. Kamishima, H. Machida, D. Watanabe, S. Nakai and M. Morishita, Application of the System Based Code concept to the determination of in-service inspection requirements, Journal of Nuclear Engineering and Radiation Science, Vol. 1, ID: 011004 (2015).
- [7] S. Takaya, N. Sasaki, and M. Tomobe, Statistical Properties of Material Strength for Reliability Evaluation of Components of Fast Reactors, Japan Atomic Energy Agency, JAEA-Data/Code 2015-002 (2015), *in Japanese*.
- [8] S. Yokoi, Y. Kamishima, D. Sadahiro and S. Takaya, Determination Methodologies for Input Data including Loads Considered for Reliability Evaluation of Fast Reactor Components, Japan Atomic Energy Agency, JAEA-Data/Code 2016-002 (2016), *in Japanese*.
- [9] T. Fujioka, T. Shimakawa, N. Miura and K. Kashima, Development and Verification of an Evaluation Method for Creep-Fatigue Crack Propagation in FBR Components, ASME-PVP, Vol. 305, pp. 395-402 (1995).
- [10] JSME S NC2-2016 Codes for Nuclear Power Generation Facilities - Rules for Design and Construction for Nuclear Power Plants -, Section II: Fast Reactor Standards (2017), *in Japanese*.